

THE EFFECT OF NODES AND FILAMENTS ON THE QUENCHING AND THE ORIENTATION OF THE SPIN OF GALAXIES

N. Malavasi¹, M. Langer¹, N. Aghanim¹, D. Galárraga-Espinosa¹ and C. Gouin¹

Abstract. Filaments and clusters of the cosmic web have an impact on the properties of galaxies, such as star-formation, stellar mass, and angular momentum. We use the IllustrisTNG simulation, coupled with the DisPerSE cosmic web extraction algorithm, to test which is the galaxy property most affected by the cosmic web and, conversely, to assess the differential impact of clusters and filaments on a given galaxy property. Results show that star-formation is the quantity that shows the strongest variation with the distances from the cosmic web features, while the direction of the angular momentum of galaxies shows the weakest trends. The direction of the angular momentum of galaxies and its use to improve our detection of the cosmic web features could be the focus of futures studies benefitting from larger statistical samples.

Keywords: large-scale structure of the Universe – Galaxies: statistics – Galaxies: evolution

1 Introduction

Both galaxy clusters (Boselli & Gavazzi 2006, 2014) and filaments (Malavasi et al. 2017; Laigle et al. 2018; Kraljic et al. 2018; Bonjean et al. 2020) affect galaxy properties, with systems in these structures being more massive and less star-forming than elsewhere. In addition, filaments also affect the acquisition of angular momentum (spin) in galaxies. Galaxies are formed with their spin parallel to the filaments of the cosmic web (Codis et al. 2015) and progressively turn massive and align their spin perpendicularly to the filaments during their evolution while flowing towards the clusters (Aragón-Calvo et al. 2007; Hahn et al. 2007). In this work (based on Malavasi et al., 2021, under review) we explore which galaxy property (mass, SFR, spin) is the most affected by cosmic web structures (clusters and filaments) and is therefore better suited to improve the detection of cosmic web elements.

2 Data and Method

We exploit 275 818 galaxies from the $z = 0$ snapshot of the TNG300-1 box of the IllustrisTNG cosmological simulation (Nelson et al. 2019), with a side of ~ 300 Mpc, defined as subhaloes with $10^9 \leq M^*/M_\odot < 10^{12}$. The filaments of the cosmic web in the simulation have been detected by Galárraga-Espinosa et al. (2020) using the Discrete Persistence Structure Extractor (DisPerSE, Sousbie 2011). We focus on three galaxy distances from the cosmic web: distance from a galaxy to the axis of the closest filament (d_{fil}), 3D distance from a galaxy to the closest node (d_{CP} , only for galaxies with $d_{\text{fil}} > 1$ Mpc), and distance from a galaxy to the node connected to the closest filament following the filaments (d_{skel} , only for galaxies with $d_{\text{fil}} < 1$ Mpc). A sketch of the three distances is shown in the left panel of Figure 1. We also focus on several galaxy properties: stellar mass M^* , SFR-related quantities (SFR, specific SFR, defined as $\text{sSFR} = \text{SFR}/M^*$, and fraction of quenched galaxies, i.e. having $\text{sSFR} \leq 10^{-11} \text{yr}^{-1}$, f_{Q}), and spin-related quantities: the angle θ between the direction of the spin vector and the local direction of the filaments (limited to $0 \leq \theta \leq 90$ deg), the fraction of parallel ($\theta \leq 30$ deg, f_{\parallel}) and perpendicular ($\theta \geq 60$ deg, f_{\perp}) galaxies, the quantity $\cos(4\theta)$ (to separate between galaxies with spin either parallel or perpendicular to the filaments, $\cos(4\theta) > 0$, i.e. galaxies having an ordered relation between spin and filament direction, and galaxies with no relation between spin and filament direction, $\cos(4\theta) < 0$), and the fraction of ordered galaxies (f_{Ord}).

¹ Université Paris-Saclay, CNRS, Institut d'Astrophysique Spatiale, 91405, Orsay, France

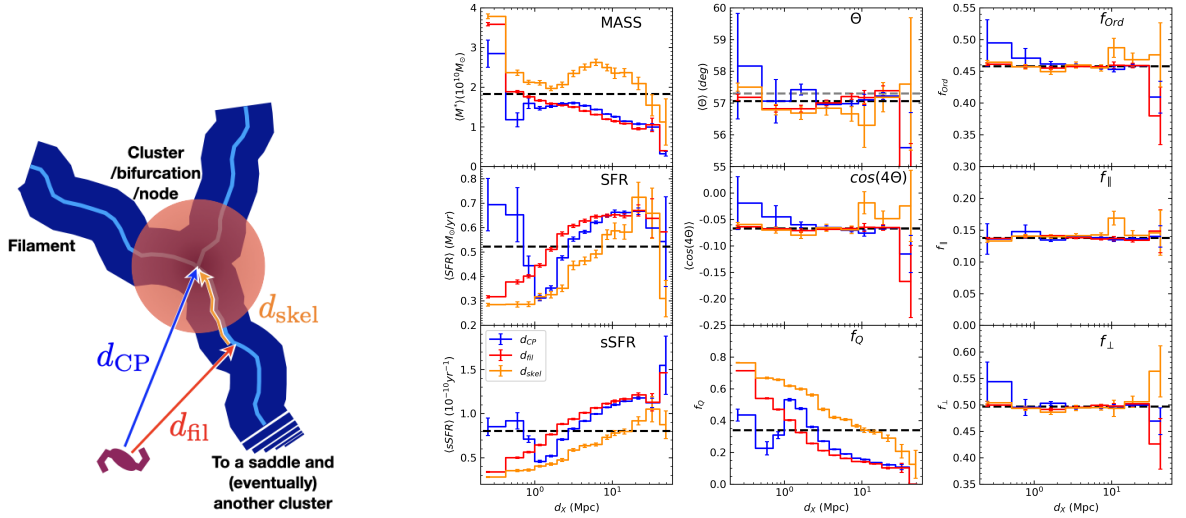


Fig. 1. Left: The three galaxy distances from the cosmic web: d_{fil} , d_{CP} , and d_{skel} . **Right:** Distributions of $\langle M^* \rangle$, $\langle \text{SFR} \rangle$, $\langle \text{sSFR} \rangle$, $\langle \theta \rangle$, $\langle \cos(4\theta) \rangle$, f_Q , f_{Ord} , f_{\parallel} , f_{\perp} in bins of d_{fil} (red), d_{CP} (blue), and d_{skel} (orange). The black dashed line in every panel is the average of each quantity in the full simulation box. For θ , the grey line is $\bar{\theta}$, computed given the expected distribution of this quantity.

3 Results and Conclusions

Figure 1 (right panel) shows the distributions of the considered quantities as a function of d_{CP} , d_{fil} , and d_{skel} . We find that SFR-related quantities allow to distinguish between d_{fil} (proxy for the accretion onto filaments) and d_{CP} and d_{skel} , proxies for the accretion onto nodes (further separated between the isotropic case and flowing inside the filaments). Mass and spin-related quantities seem to allow only for a distinction between d_{CP} and d_{fil} with respect to d_{skel} . The distributions of SFR-related quantities are those that show the largest variation with respect to each distance, a further confirmation that they are the best tracers for d_{CP} , d_{fil} , and d_{skel} . Spin-related quantities show the lowest amount of variation and are therefore the worse tracer. However, SFR-related quantities show also a large dependence on the local environment of galaxies, which may prevent their use as tracers to improve the detection of the cosmic web. On the other hand, spin related quantities are more robust with respect to the effect of local density. Although the strength of the signal of the recovered trends is lower, their use could provide a detection of the cosmic web in a way more independent from the local density.

This research has been supported by the funding for the ByoPiC project from the European Research Council (ERC) under the European Union’s Horizon 2020 research and innovation programme grant agreement ERC-2015-AdG 695561.

References

- Aragón-Calvo, M. A., van de Weygaert, R., Jones, B. J. T., & van der Hulst, J. M. 2007, ApJ, 655, L5
 Bonjean, V., Aghanim, N., Douspis, M., Malavasi, N., & Tanimura, H. 2020, A&A, 638, A75
 Boselli, A. & Gavazzi, G. 2006, PASP, 118, 517
 Boselli, A. & Gavazzi, G. 2014, A&A Rev., 22, 74
 Codis, S., Pichon, C., & Pogosyan, D. 2015, MNRAS, 452, 3369
 Galárraga-Espinosa, D., Aghanim, N., Langer, M., Gouin, C., & Malavasi, N. 2020, A&A, 641, A173
 Hahn, O., Carollo, C. M., Porciani, C., & Dekel, A. 2007, MNRAS, 381, 41
 Kraljic, K., Arnouts, S., Pichon, C., et al. 2018, MNRAS, 474, 547
 Laigle, C., Pichon, C., Arnouts, S., et al. 2018, MNRAS, 474, 5437
 Malavasi, N., Arnouts, S., Vibert, D., et al. 2017, MNRAS, 465, 3817
 Nelson, D., Springel, V., Pillepich, A., et al. 2019, Computational Astrophysics and Cosmology, 6, 2
 Sousbie, T. 2011, MNRAS, 414, 350